

The point spread function of electrons in a magnetic field, and the β -decay of free neutrons

D. Dubbers¹, B. Märkisch¹, F. Friedl¹, H. Abele^{1,2}

¹Physikalisches Institut der Universität, Philosophenweg 12, D-69120 Heidelberg, Germany

²Technische Universität München, D-85748 Garching, Germany

(Dated: December 01, 2008)

ABSTRACT

When a uniform magnetic field is used to guide electrons from a β -emitter to a detector, the electrons on the detector are distributed over an area whose size is larger than the size of the source by up to four radii of gyration, and more if also backscattered electrons are registered. This blurring of the image of the electron source can be described by a suitable point spread function (PSF). This rather general problem is investigated in the context of newly developed neutron β -decay spectrometers. We derive this 'magnetic' PSF for an active neutron decay volume coupled to an electron detector by a magnetic field. We then investigate the effect of limited detector size on measured neutron decay correlation parameters like the β -decay asymmetry. To our surprise we find that in a typical spectrometer setup, even when detector size is as small as the size of the source, then this will change the asymmetry by less than 10^{-3} .

PACS: 13.30.Ce, 29.27.Eg, 29.30.-h, 29.30.Dn.

Keywords: cold neutrons, beta decay, electron detectors

1. Introduction

In nuclear spectroscopy, magnetic fields are frequently used to guide charged particles onto their detectors. This technique permits the use of relatively small detectors for full 2π solid angle of detection, and even 4π , when two detectors are installed in the magnetic field opposite to each other on both sides of the source. In high precision β -spectroscopy with polarized sources, this method has the additional advantage that the magnetic field permits a very clean cut between those electrons emitted under angles $\theta < \pi/2$ and those emitted under $\theta > \pi/2$ with respect to the local field direction, and hence to the nuclear polarization vector, which everywhere is aligned along the local field. This makes the measurement of correlation coefficients, like the parity non-conserving β -asymmetry A , the neutrino asymmetry B , or the electron-neutrino correlation coefficient a , independent of the precise positioning of the detectors, and also independent of the precise local field direction. This advantage was already pointed out in the seminal paper [1] on parity violation.

In particular, most modern spectrometers for the study of neutron β -decay correlations in use (*a*SPECT, PERKEO, UCNA) or under development (abBA, aCORN, Nab, PANDA, PERC, PNPI) use magnetic fields to guide the neutron decay products onto the electron and/or proton detectors, for references see Ref. [2,3]. Magnetic guide fields are also used in several experiments on the neutron lifetime [3]. These experiments now all aim at measurement accuracy of 10^{-3} or better [3-6].

Evidently, the detectors used must be large enough to accept all significant events. To be safe, in view of the high accuracy aimed at, one would, all around the core image of the source on the detector, add an area which accepts all incoming electrons up to the maximum occurring diameter of gyration. When electrons are backscattered on one detector and registered in a second detector opposite to the first one, then a new helical trajectory is started which, in the worst case, will require, all around the detector, another area one maximum diameter of gyration wide, and so on. To give an example: the large new PERKEO III neutron decay instrument [7] has a maximum neutron beam diameter of 16 cm, and with a guide field of $B_0 = 0.15$ Tesla, the maximum diameter of electron and proton gyration reaches $2R = 5$ cm in the neutron beam, and $2R = 7$ cm on the detector, which is in a lower field of 0.09 Tesla. Typical electron backscattering coefficients are 10% to 20%. An additional safety margin of two times or even four times 7 cm in each dimension would require a rather large detector, with negative consequences for energy resolution, background sensitivity, and size of the magnet coils.

The investigation of this problem seems to be a rather elementary exercise. However, the problem requires six successive integrations over partly diverging distributions, and the result was, for us, both unexpected and comforting. As charged particle detection in a magnetic field is a widespread technique, we think that our results might be of interest to a wider community.

2. The charged particle source

To be specific, we shall treat the case of an electron source, although the results are valid for charged particle emission in general. We first define the brightness of the electron source

$$B = \frac{\partial^2 \Phi}{\partial E \partial \Omega}, \quad (1)$$

(given, for instance, in units of $\text{cm}^{-2}\text{s}^{-1}\text{keV}^{-1}\text{sr}^{-1}$) with electron kinetic energy E , solid angle of emission Ω , and electron flux density Φ , in close analogy to neutron brightness B_n , neutron flux density Φ_n , etc., see for instance Ref. [8].

For an extended electron source in an external magnetic field B_0 , electron brightness B depends on position \mathbf{x} , electron kinetic energy E , and polar angle of emission θ . In the case of free neutron decay, B can be factorized to

$$B(\mathbf{x}, E, \theta) = b_0(\mathbf{x}) F(E) w(E, \theta), \quad (2)$$

with the allowed β -spectrum $F(E) = (E_0 - E)^2 E^{1/2} (E + 2m)^{1/2} / (E + m)$, with electron rest energy $m = 511$ keV, and endpoint energy $E_0 = 783$ keV for neutron decay. Alternatively, if a conversion electron calibration source is used, $F(E)$ can be a collection of δ -functions.

For isotropic electron emission, the angular dependence is $w(E, \theta) \equiv 1$. For the measurement of correlation parameters like the β -decay asymmetry A (for the neutron $A \approx 0.12$), the angular distribution is

$$w(E, \theta) = 1 + AP_n \beta \cos \theta, \quad (4)$$

with neutron polarization P_n , and electron velocity $\beta = v/c$ in terms of the speed of light. In a magnetic field, the mean $\langle \cos \theta \rangle = 1/2$. The measured asymmetry signal $A_m = AP_n \beta$ is obtained by flipping the neutron polarization periodically between $+P_n$ and $-P_n$. A_m depends on electron energy E via $\beta = v/c = E^{1/2} (E + 2m)^{1/2} / (E + m)$.

For an electron source in a magnetic field, the radius of gyration for emission under $\theta = \pi/2$ is $r_0(E) = E^{1/2}(E + 2m)^{1/2}/(ceB_0)$, with electron charge e and momentum p . For emission under polar angle θ (relative to the B_0 -field direction) the radius of gyration is

$$r(E, \theta) = r_0(E) \sin \theta. \quad (7)$$

In neutron β -decay, electron brightness B is proportional to the local neutron density ρ_n , which, for a neutron beam, is proportional to the local neutron capture flux density Φ_n (also called the thermal equivalent flux). Most neutron decay correlation studies use cold neutrons from a neutron guide (aligned along the z -axis) of rectangular cross-section (typical area 100 cm^2). The transverse neutron beam profile then is separable in the coordinates x and y as

$$\Phi_n(x, y) = \Phi_{n0} \phi_n(x) \phi_n'(y), \quad (8)$$

with dimensionless distributions $\phi_n(x)$ and $\phi_n'(y)$, cf. Section 4. This translates into a separable electron brightness profile across the neutron beam

$$B(x, y) = B_0 b(x) b'(y). \quad (9)$$

Here and in the following, neutron beam parameters carry the subscript n , beam parameters with no such subscript refer to the electron beam; we also shall drop the pre-factors Φ_{n0} and B_0 .

3. The magnetic point spread function

The neutron decay spectrometers under discussion typically have an active neutron decay volume ranging from several cm^3 to many dm^3 . Electrons originating in an infinitesimal volume element, located at position \mathbf{x} within the source volume, are guided by the B_0 -field and projected on the detector within a circular area of diameter four times the maximum occurring gyration radius R . In general, the response function of an imaging system to a point object or point source is called the point spread function (PSF) of the system. Our beam-optical system then consists of an electron point source at \mathbf{x} , a magnetic guide field as imaging system, and an electron detector; the position dependent distribution of electrons on the detector will then be called the magnetic PSF.

The electron brightness profile on the detector along the axis x then is derived from the initial electron brightness profile $b(x) \propto \phi_n(x)$ within the neutron decay volume by

$$b(x, E, \theta) \propto F(E) w(E, \theta) \int_{x-2r}^{x+2r} f_1(x-x', E, \theta) \phi_n(x') dx', \quad (10)$$

where $f_1(x-x', E, \theta)$ is the magnetic PSF for electron brightness, and similarly for $b'(y, E, \theta)$. Here it is assumed, without loss of generality, that the field B_0 is applied along the neutron beam axis z , like in PERKEO III.

To find the point spread functions for the brightness B , and, after successive integration, for the electron flux spectrum $\partial\Phi/\partial E$ and the electron flux density Φ , we first regard the helical trajectories of electrons emitted from the decay position (x', y') under polar angle θ and azimuth angle φ . In the (x, y) -plane, the electrons move on a circle of radius r (full line in Fig. 1) about a guiding center (x'', y'') , which is located on a circle of radius r (dashed line) about the origin (x', y') . The projection of this motion onto the x -axis is $x-x' = x'' + r \cos\chi$, with angle χ as seen from (x'', y'') , and

$$\frac{dx}{d\chi} = r \sin \chi = \sqrt{r^2 - (x-x'-x'')^2}, \quad (11)$$

with $r = r(E, \theta)$, and with x'' counted from the location x' where neutron decay occurred.

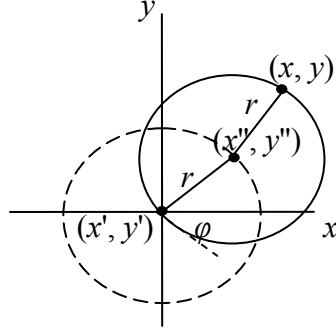


Fig. 1: Gyration of electrons in a magnetic field B_0 applied along z . The electrons are emitted at (x', y') under azimuth angle φ and gyrate (full circle) about the guiding center (x'', y'') located on the dashed circle.

Under the uniform circular motion of the electrons, the fraction of electrons on line element $ds = r d\chi$ is $dn = d\chi/(2\pi)$. The distribution of electrons along x , normalized to 1, then becomes, for a given x'' ,

$$f_0(x - x') = 2 \frac{dn}{dx} = 2 \frac{dn}{d\chi} \frac{d\chi}{dx} = \frac{1}{\pi \sqrt{r^2 - (x - x' - x'')^2}}, \quad (12)$$

which diverges at $x - x' - x'' = \pm r$. This distribution is shown in Fig. 2a) for $x'' = 0$ and maximum radius of gyration, which is $R \equiv r_0(E_0) = 2.6$ cm for neutron decay in the $B_0 = 0.15$ Tesla field of PERKEO III.

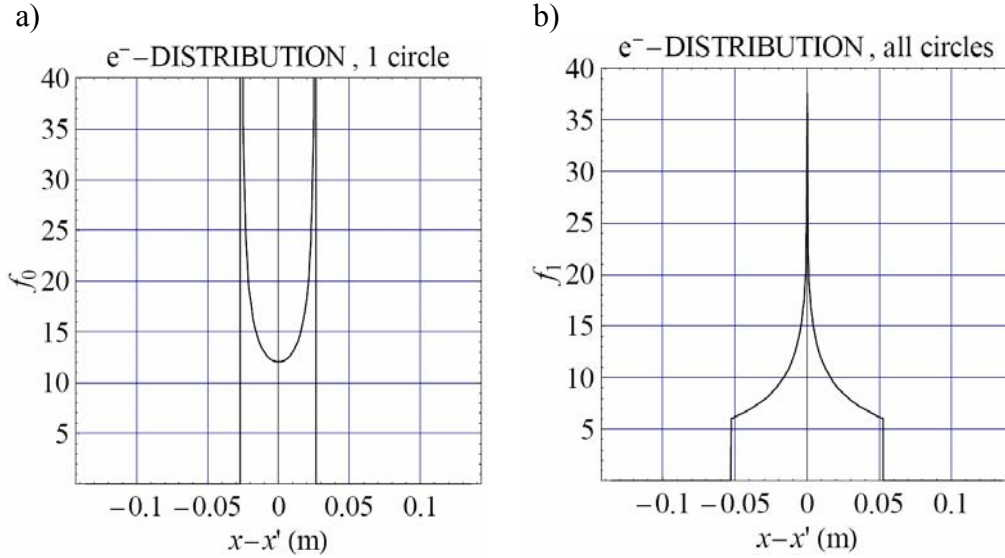


Fig. 2: Distribution of electrons along the transverse x -axis, for neutron β -decay at x' in the field $B_0 = 0.15$ T, for the maximum occurring radius of gyration $R = 2.6$ cm,

a) for electrons emitted in x -direction ($\varphi = 0$), using (12) for $x'' = 0$,

b) averaged over azimuth angles φ , using (14).

The abscissa goes over the full width of the electron distribution in the active decay volume of PERKEO III.

We then integrate f_0 over azimuth angles φ of electron emission, that is over x'' with $d\varphi = (d\varphi/dx'') dx''$. A given position $x'' = r \cos\varphi$ of the guiding center then has the weight $d\varphi/dx'' = (r^2 - x''^2)^{-1/2}/\pi$, and integration over x'' gives the magnetic PSF for electron brightness for a given radius $r = r(E, \theta)$, to be inserted in (10). For $x - x' > 0$,

$$f_1(x - x', E, \theta) = \frac{1}{\pi^2} \int_{-r+x-x'}^r \frac{1}{\sqrt{r^2 - (x - x' - x'')^2}} \frac{1}{\sqrt{r^2 - x''^2}} dx'', \quad (13)$$

This integral can be expressed in terms of elliptic integrals in various ways. Using relations like $K(1/m) = m^{-1/2} F(\operatorname{arccsc}(m^{1/2}), m) = m^{1/2} K(m)$ for the complete and incomplete elliptical integral of the first kind K and F , all these expressions can be reduced to the simple form

$$f_1(x - x', E, \theta) = \frac{1}{\pi^2 r} K\left(1 - \frac{(x - x')^2}{4r^2}\right) \quad (14)$$

for $|x - x'| < 2r$, and $f_1 = 0$ otherwise, which holds for both signs of $x - x'$. We use the notation $K(m)$, another popular notation being $K(k)$ with $k^2 = m$. The use of K , which is a built-in function in most mathematical packages, is much preferred over a numerical integration of the strongly divergent integrand of (13).

Eq. (14) is our result for the magnetic PSF f_1 for a given radius r of gyration, and is displayed in Fig. 2b) for $r = R$. The pole now has moved to the center x , which is due to the fact that all circles pass through the point (x', y') where neutron decay occurs. This pole is much milder than the pole of Fig. 2a), and further numerical integration is straightforward.

We next integrate f_1 numerically over θ

$$f_2(x - x', E) = \frac{1}{\pi^2 r_0(E)} \int_{\arcsin \Delta}^{\pi/2} K(1 - \Delta^2 / \sin^2 \theta) w(E, \theta) d\theta \quad (15)$$

with $\Delta = (x - x')/(2r_0(E))$. Fig. 3a) shows the magnetic PSF f_2 for isotropic emission $w \equiv 1$ at neutron end point energy $E = E_0$. Fig. 3b) shows the energy average of f_2 over the β -spectrum.

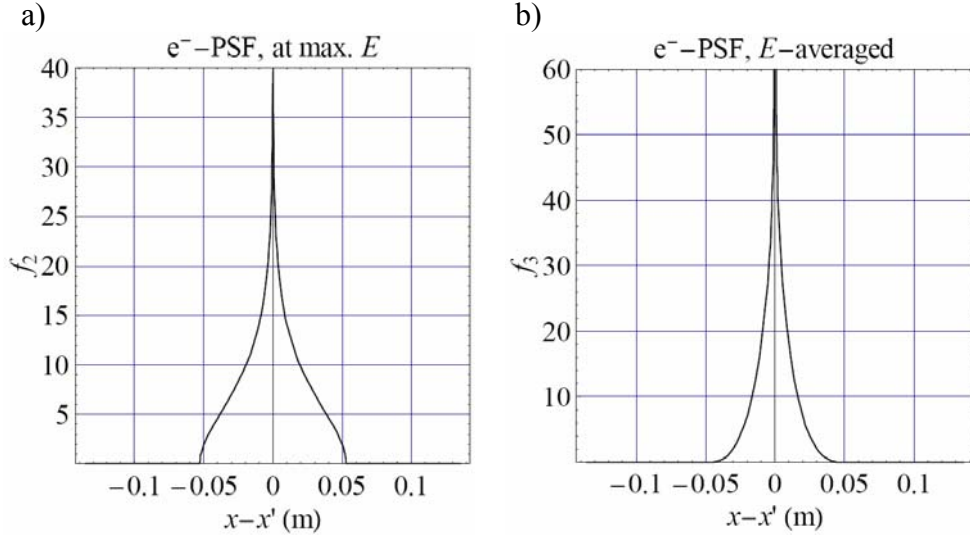


Fig. 3: Magnetic point spread function for isotropic electron emission ($w \equiv 1$),
a) at β -endpoint energy $E = E_0$, using (15),
b) averaged over neutron β -decay energies, using (19).

4. Electron beam profiles in neutron decay

The exit port of a neutron guide emits neutrons isotropically up to a cut-off angle $\theta_c = k_{xc}/k = \lambda/\lambda_c$, which is the critical angle of total neutron reflection off the inner coating of the neutron guide. Here λ and $k = 2\pi/\lambda$ are the neutron de Broglie wavelength and wave number, and $\hbar k_{xc} = h/\lambda_c$ is the transverse neutron momentum at θ_c . In Ref. [8] this neutron distribution was checked experimentally to hold rather well also for the "ballistic supermirror" neutron guide H113 of the fundamental physics beam line PF1 of ILL, Grenoble, where PERKEO III is installed. Hence, for a given position \mathbf{x} within the neutron decay volume, the neutron flux $\Phi_n(\mathbf{x})$ is proportional to the solid angle Ω_n under which the neutron source is seen from \mathbf{x} , which also holds if the source is seen through a neutron collimator. For a collimator made of successive neutron absorbing orifices with rectangular openings of varying size, the flux profile (8) of the diverging neutron beam is $\phi_n(x)\phi_n'(y) \propto \Omega_n = \theta_x\theta_y$. At a given distance z from the guide exit, the limiting angle $\theta_x(z)$ can be calculated numerically with a single line of code

$$\theta_x(z) = \text{Min}(\theta_c, \theta_1^+, \theta_2^+, \dots) - \text{Max}(-\theta_c, \theta_1^-, \theta_2^-, \dots), \quad (16)$$

cf. Fig. 4, and similarly for $\theta_y(z)$.

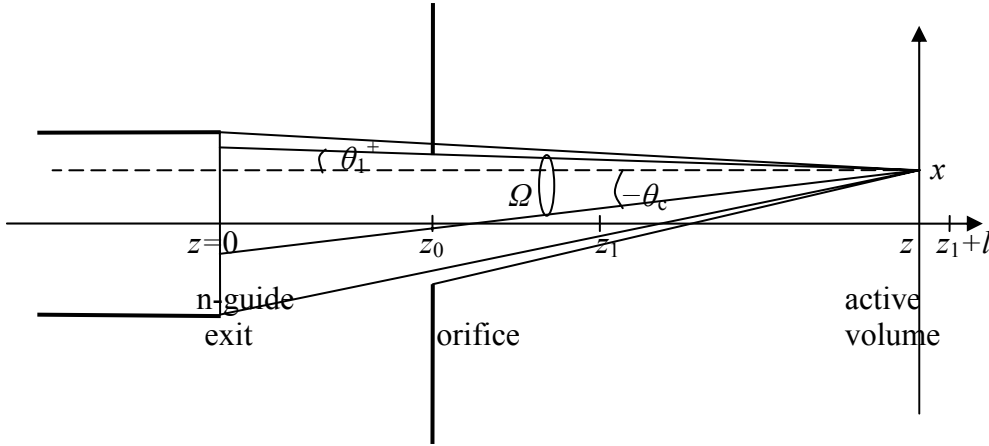


Fig. 4: Solid angle Ω for the calculation of neutron flux density profiles, using (16).

The neutron flux originating along one magnetic field line must then be added up, in our case along the neutron beam axis z , which can be done numerically in rather large steps of dz to give

$$\phi_n(x) \propto \int_{z_1}^{z_1+l} \theta_x(z) dz, \quad (17)$$

where l is the length of the decay volume.

In PERKEO III, the neutron collimator is made of four orifices, the first one with a $6 \times 6 \text{ cm}^2$ window on the exit port of the cold-neutron guide ($z = 0$), the last one with a $5 \times 5 \text{ cm}^2$ window at $z_0 = 4.2 \text{ m}$. In the pulsed neutron mode, with neutron wavelength $\lambda = 0.6 \text{ nm}$ and critical angle $\theta_c = 0.016$, this last orifice is fully illuminated. The active decay volume begins at $z_1 = 6.2 \text{ m}$ and has a length $l = 2.0 \text{ m}$. The width of the neutron beam at the end of the decay volume is geometrically limited by the collimator to $b = \pm 8.3 \text{ cm}$. The dashed line in Fig. 5 shows the calculated neutron beam profile $\phi_n(x)$ for this case, set to 1 at $x = 0$. The maximum width of the neutron beam at the end of the decay volume is geometrically limited to $2b = 16.6 \text{ cm}$.

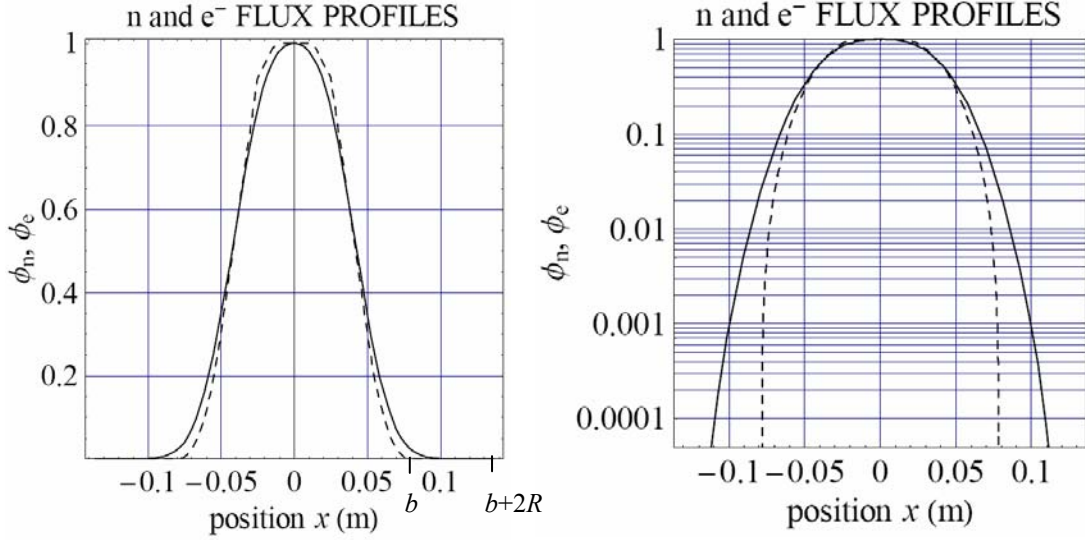


Fig. 5: Neutron flux profile (17) (dashed line) and electron flux profile (20) (full line), on a linear and a logarithmic scale, calculated for the neutron beam configuration of PERKEO III.

The profile of the beam of decay electrons then is calculated by folding $\phi_n(x)$ with the electron PSF, either before or after integration over electron energy. In the first case one obtains the electron profile separately for each electron energy E ,

$$\frac{\partial \phi(x)}{\partial E} = F(E) \int_{-b-2R}^{b+2R} f_2(x-x', E) \phi_n(x') dx'. \quad (18)$$

In the second case, after integration over electron energy

$$f_3(x-x') = \int_0^{E_0} F(E) f_2(x-x', E) dE, \quad (19)$$

the total electron flux profile is

$$\phi(x) = \int_{-b-2R}^{b+2R} f_3(x-x') \phi_n(x') dx', \quad (20)$$

where $2(b+2R) = 27$ cm is the maximum width of the electron beam, as compared to the maximum width $2b = 16.6$ cm of the neutron beam. The same can be done for $\phi'(y)$, to obtain the electron distribution $\Phi(x, y) = \phi(x)\phi'(y)$ on the detector. All electrons originating within a radius of $2R = 5$ cm may contribute to the flux Φ at position (x, y) . If the electron detector is installed in a magnetic field B_1 lower than the field B_0 in the neutron decay volume, then this distribution must, under adiabatic transport from B_0 to B_1 , be stretched by a factor $(B_0/B_1)^{1/2}$. For PERKEO III, this factor is $(1.5/0.9)^{1/2} = 1.3$.

The full lines in Fig. 5 show the electron distribution $\phi(x)$ for isotropic neutron β -decay. Remarkably, the half-width of the electron distribution remains about the same as that of the neutron distribution, and the widening of the tails is considerably smaller than the maximum diameter of gyration $2R = 5$ cm. To study the tails of the electron distribution in more detail, the distribution is shown in Fig. 5 also on a logarithmic scale. Already at 10 cm distance from the center $x = 0$ of the neutron beam, that is 2 cm outside the geometric neutron limits $\pm b$, the electron flux has dropped to below 10^{-3} of its peak value.

More informative is the integrated flux of electrons, that is the electron intensity Δi in the tails of this distribution, beyond a given distance x_d from the center of the distribution, as compared to the intensity i within x_d , that is the quantities

$$\Delta i(x_d) = \int_{x_d}^{b+2R} \phi(x) dx \text{ and } i(x_d) = \int_0^{x_d} \phi(x) dx. \quad (21)$$

In PERKEO III, the integrated intensity $\Delta i(b)$ outside the geometric limits $\pm b$ of the neutron beam is $4 \cdot 10^{-3}$ of total intensity $i(b+2R)$, and drops to below 10^{-4} another two centimeter further out.

5. Implications for neutron decay correlations

Our main interest, however, is not in the effect of these electron losses on intensities, but on the neutron decay correlation signal. The distribution of the measured asymmetry signal A_m over the area of the detector is

$$A_m(x, y) = \frac{\Phi^+(x, y) - \Phi^-(x, y)}{\Phi^+(x, y) + \Phi^-(x, y)}, \text{ with } \Phi^\pm(x, y) = \phi^\pm(x) \phi'^\pm(y), \quad (22)$$

where the \pm signs indicate the state of neutron polarization.

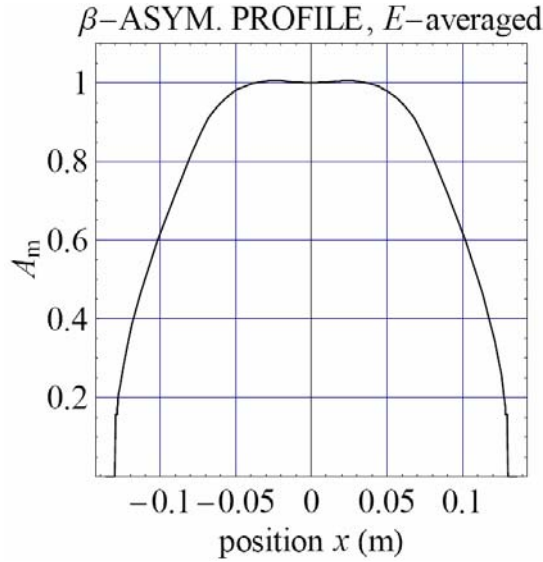


Fig. 6: Profile (22) of β -decay asymmetry across the n-beam, with $y = 0$.

Fig. 6 shows the profile $A_m(x, 0)$, set to 1 at $x = 0$. A_m is position dependent because only the electrons with large radii reach the outer tails of the electron distribution. Radii are large for large electron energies, where the asymmetry A_m is large, and for electron emission angles near $\theta = \pi/2$, where the asymmetry A_m vanishes. Off center, A_m increases first by up to $5 \cdot 10^{-3}$ at $x = \pm 3$ cm. At the geometric limit b of the neutron beam, A_m has decreased by 20%. At the outer limit $b+2R$ of the electron distribution, the asymmetry signal disappears altogether, because only electrons emitted under $\theta = \pi/2$ with vanishing A_m can contribute there.

At first sight, these effects look frightening in view of the accuracy of A we are aiming at. However, we have not yet taken into account that there is almost no intensity in the tails. So how strongly is the measured asymmetry affected when electrons in the outer tails of the distribution are not registered? The total intensity within a detector area limited by $|x| \leq x_d$ and $|y| \leq y_d$ is

$$I^\pm(x_d, y_d) = \int_0^{x_d} \phi^\pm(x) dx \int_0^{y_d} \phi'^\pm(y) dy = i^\pm(x_d) i^\pm(y_d) \quad (23)$$

which, for a square distribution with $x_d = y_d$, equals $i^\pm(x_d)^2$, cf. (21). The asymmetry as a function of the area x_d^2 of electron detection then is

$$A_m(x_d^2) = \frac{[i^+(x_d)]^2 - [i^-(x_d)]^2}{[i^+(x_d)]^2 + [i^-(x_d)]^2}. \quad (24)$$

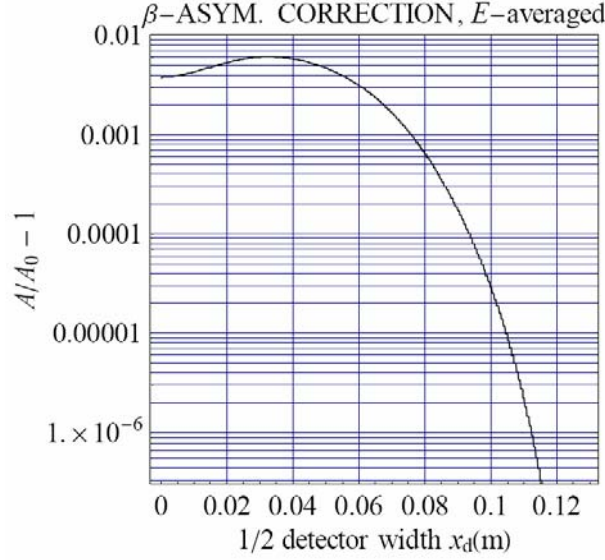


Fig. 7: Corrections to the β -asymmetry due to limited detector area x_d^2 , using (24). The geometric limit of the neutron beam lies at $x_d = 0.08$ m, and the geometric limit of the electron beam lies at the end of the abscissa at $x_d = 0.136$ m.

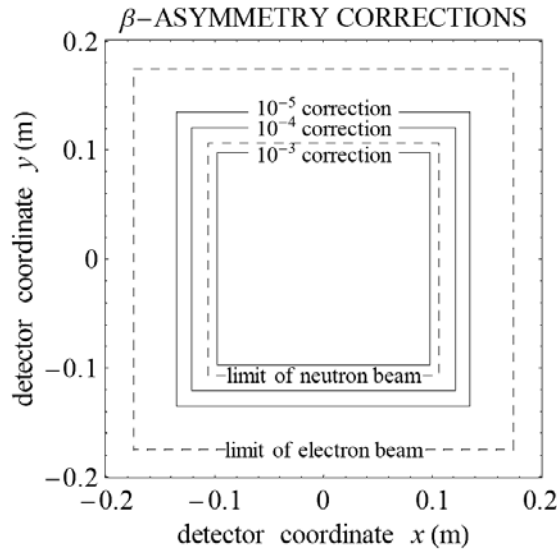


Fig. 8: Corrections to the β -decay asymmetry, for various detector areas (full lines). The geometric limits of the neutron beam projection and the beam of decay electrons (no backscattering) are also shown (dashed lines). The x - and y -scales are stretched by a factor 1.3, as compared to the previous figures, to take into account the widening of the electron beam in the lower magnetic field at the detector site.

Fig. 7 shows the change of the asymmetry signal $A_m(x_d^2)/A_m(\infty) - 1$ if electron detection is limited to the inner detector region $|x| < x_d$ and $|y| < x_d$. To our surprise, we find that, even if

we lose all electrons that hit the detector outside the neutron confinement of $|b| = 8$ cm, the effect on the asymmetry is much smaller than the lowest present experimental error of several 10^{-3} , and drops very rapidly with every cm of safety margin added. This further shows that we can also neglect additional widening of the electron beam due to backscattering on the detector, which must occur near glancing incidence and go back into the incoming direction to make a sizeable effect. In Fig. 8 the data of Fig. 7 are used to indicate, in the plane of the detector, what detector size corresponds to a given level of correction in the β -asymmetry A .

In summary, we find that in angular correlation experiments which use magnetic guide fields to transport the charged decay particles to the detectors, one can in most cases safely neglect the electrons which gyrate outside of the active decay volume. For PERKEO III this means that the size of the electron or proton detectors, and with it the size of the magnet coils, can safely be decreased to about one half of their width, or to one quarter of their area, as compared to the area needed to intercept all events. Alternatively, the cross-section of the neutron beam and, with it, the event rate can be increased by the same amount, without impeding the quality of the instrument.

References

- [1] T.D. Lee, C.N. Yang, Phys. Rev. 104 (1956) 254.
- [2] D. Dubbers, et al., Nucl. Instr. and Meth. A (2008), A 596 (2008) 238.
- [3] International Workshop on Particle Physics with Slow Neutrons, Institut Laue Langevin, Grenoble, France (2008), Nucl. Instr. and Meth. A, in print.
- [4] H. Abele, Prog. Part. Nucl. Phys. 60 (2008) 1.
- [5] N. Severijns, M. Beck, O. Naviliat-Cuncic, Rev. Mod. Phys. 78 (2006) 991.
- [6] J.S. Nico, W.M. Snow, Annu. Rev. Nucl. Part. Sci. 55 (2005) 27.
- [7] B. Märkisch, Doctoral Thesis, Heidelberg University, 2006 / <http://www.u-b.uni-heidelberg.de/archiv/6927/S>, and Ref. [3].
- [8] H. Abele, et al., Nucl. Instr. and Meth. A 562 (2006) 407.